Molecular Signature Of Subtypes Of Renal Cell Carcinomas And Immunotherapy Strategy

JiaNing Guo
tianjin institute of urology
Xi Yu
Tianjin Institute of Urology
Bin He
Tianjin Institute of Urology
ShengLai Liu
Tianjin Institute of Urology
Ning Jiang (jiangning@bjmu.edu.cn)
Tianjin Institute of Urology

Research Article

Keywords: RCC, Tumor immunity, Immunogenomic profiling, Immunotherapy

Posted Date: March 9th, 2022

DOI: https://doi.org/10.21203/rs.3.rs-847344/v2

Abstract

Purpose: Classified immunogenomic profiling based on therapeutic responses in RCC subtypes.

Methods: Tumors from RCC patients from The Cancer Genome Atlas (TCGA) cohort were analyzed, and genomic profiling was performed. We classified RCC on the basis of the immunogenomic profiling of 29 immune signatures.

Results: We investigated the transcriptional changes of three RCC subtypes by RNA-seq. Gene ontology (GO) identify specific gene signatures differed significantly between KIRC, KIRP and KICH related to the distinct pathways. Site of origin within the nephron was one major determinant in the molecular and immune classification, reflecting differences between three subtypes. The Immunity High KIRC and KIRP subtype was enriched not only in immune signatures, but also including PD-L1 expression signaling, NF-kappa B signaling pathway, JAK-STAT signaling pathway and Cell cycle signaling pathway. KICH was a distinct disease that shared little genomic characteristics with KIRC and KIRP.

Conclusions: The identification of RCC subtypes based on immune signatures has potential clinical implications for RCC treatment. It is imaginable that patients with higher immunity subtype of KIRC and KIRP would be more likely to respond to anti-PD-1/ PD-L1 therapy than patients with KICH subtype. CCL21 and CCL25 might be a potential target for KICH therapy.

1. Introduction

Renal cell carcinomas (RCC) comprised 2-3% of all non-cutaneous malignant neoplasms and was the sixth most common cancer in men and the eighth most common cancer in women in 2019 [1, 2]. Renal epithelial tumors arised from renal tubules and included three main subtypes: clear cell RCC (KIRC) accounted for 75% of RCC, papillary RCC (KIRP) accounted for 15%~20%, and chromophobe RCC (KICH) represented 5% [3]. Although surgical resection was common for Patients with RCC, uncontrolled tumor progression and death still occured and RCC was poor response to conventional chemotherapeutics and radiation [4, 5]. Notably, RCC subtypes were associated with different histology, biological behaviors, prognosis, and responses to therapy. Thus, more effective systemic treatments for RCC subtypes patients are needed to guide treatment decisions.

Recently, cancer immunotherapy with the use of immune checkpoint inhibitors (ICIs) has been reported as an appreciated therapeutic approach for the tumors including RCC[6, 7]. Indeed, many experimental and clinical trials had explored the possibility of treating RCC patients with immunotherapy and expression of programmed death ligand 1 (PD-L1) in the tumors of patients[8–11]. However, some patients were insensitive to ICIs, this suggested that not all RCC patients could respond to immunotherapy. In fact, tumor mutation burden (TMB), neoantigen expression, PD-L1 expression, PBRM1 loss and deficient DNA mismatch repair, have been associated with cancer immunotherapeutic responsiveness [12–18]. Therefore, a more accurate classification system based on a comprehensive immune-related genes is deeply needed to improve prognosis accuracy and direct clinical practice.

In this study, we identified the common and specific molecular characteristics of subtype-specific treatment and management strategies for these cancer patients. The identification of immune signature-associated RCC subtypes may facilitate the optimal selection of RCC patients responsive to immunotherapy.

2. Material And Methods

2.1 Patient Cohort

We used publicly available level 3 data of TCGA in this study. mRNA expression data based on RNAseq of the TCGA samples were downloaded from the UCSC Cancer Browser. mRNA expression data, which were generated using the Illumina HiSeq V2 platform, are presented as reads per kilobase per million (RPKM) and transformed into log 2 values for analysis. We obtained the samples with Kidney Chromophobe (KICH, n=85), Kidney Clear Cell Carcinoma (KIRC, n=606), and Kidney Papillary Cell Carcinoma (KIRP, n=321). Two validation cohorts were used from GEO database (GSE15641 and GSE19949/GSE12090), of which GSE15641 were about 49 samples (KIRC, n=32; KIRP, n= 11; KICH, n=6) and GSE19949 (KIRC, n=79; KIRP, n=20; KICH, n=9).

2.2 Functional enrichment analysis

In order to investigate difference in potential biological role between tumor and normal tissue in KICH, KIRC, and KIRP, we used the DEGs obtained using limma and edgeR package of R to perform exploration with filtering criteria of FDR<0.01 and |logFC|>1. clusterProfiler of R was used to further functional enrichment analysis[19]. Only GO categories of ‘Biological Process’ were considered. Functional annotation with *P*-value <0.05 was considered be statistically significant.

2.3 Infiltrating Immune Cell Quantification

To determine the degree of immune cell infiltration in tumor, we performed the single-sample gene-set enrichment analysis (ssGSEA) score, which applied 28 expression-based gene signatures of immune cell populations to individual tumor samples[20]. The immune infiltration score, stromal infiltration score and tumor purity for each RCC sample was calculated using ESTIMATE. MCP-counter computational algorithms were also used to characterize immune cell composition in both tumor and normal tissue[21].

2.4 Statistical analysis

Correlations were evaluated using the Spearman correlation test. The significance of the differences between continuous variable (immune infiltration level and chemokine expression) and categorical variable (RCC subtypes) was calculated by the Wilcoxon rank-sum test. Statistical analyses were performed using R software and were deemed to be significant with a P-value <0.05 (two-sided).

3. Results

3.1 Gene Ontology and Canonical Pathway Analysis in three subgroups

We explore the biological and functional difference in three subgroups based on the differential expressed genes, especially the immune response and tumor microenvironment. Firstly, a total of 5699 DEGs were calculated in KIRC relative to normal tissue, including 3804 up-regulated and 1895 down-regulated genes(Fig. 1A); In KIRP relative to normal tissue, 4896 genes were differentially expressed including 2899 up-regulated and 1997 down-regulated genes(Fig. 1B); 5759 of genes significantly differentially expressed in KICH relative to normal tissue, with 2685 up-regulated and 3074 down-regulated genes (Fig. 1C). Further exploration, a total of 1208 intersection genes among the three subgroups were screened including 607 up-regulated and 601 down-regulated genes (Fig. 1D).

Among all the GO-terms, only 786 (27.7%) intersected among the three subgroups (Supplemental Figure1A). GO-enrichment analysis revealed that among the DEGs were those involved in cell differentiation, meiotic cell cycle, cell maturation, DNA transcription, growth factor activity, leukocyte migration, and DNA repair. These processes were involved in cancer progress and play critical role in the initiation and promotion of tumorigenesis (Supplemental Figure1B). When we looked at the GO-terms in each subgroup of RCC, we noticed that, immune response process was enriched in KIRC, such as T cell differentiation, T cell activation, cell killing, leukocyte proliferation, lymphocyte proliferation and cytokine secretion (Supplemental Figure1C). What's more, we found GO-terms in KIRP were related with metabolism of organic and inorganic matter, such as response to lipopolysaccharide and carbohydrate binding. Interestingly, the immune response also was enriched in KIRP, such as interleukin-1 production, mononuclear cell proliferation and mononuclear cell migration (Supplemental Figure1D). In KICH, more biological functions were seemed to be involve in regulation of synaptic plasticity, kidney morphogenesis, axoneme, and metabolic process (Supplemental Figure1E).

Pathways analysis identified 73, 77 and 73 altered pathways in KICH, KIRC, and KIRP, respectively (FDR<0.05) (Supplemental Figure2A). The top 10 pathways of each subgroups were screened compared with normal tissue. Among them, a total of 32 pathways were common to each subgroup. Cytokine-cytokine receptor interaction, cell adhesion molecules (CAMs), calcium signaling pathway, ECM-receptor interaction, steroid hormone biosynthesis and PPAR signaling pathway were the most significant changed pathways in each subgroup of RCC(Supplemental Figure2B). The tope dysregulated pathways detected in KIRC were more activated mainly associated with immune response (Supplemental Figure2C), such as Th1 and Th2 cell differentiation, Allograft rejection, Graft-versus-host disease, Th17 cell differentiation, Natural killer cell mediated cytotoxicity. Besides, the cancer-related signal pathways also were more activated compared with normal tissue, such as Transcriptional misregulation in cancer, Chemokine signaling pathway, JAK-STAT signaling pathway, and Rap1 signaling pathway. We found the KEGG pathways was only enriched in KIRP (Supplemental Figure2D), such as p53 signaling pathway, cGMP-PKG signaling pathway, Primary immunodeficiency, PI3K-Akt signaling pathway, PI3K-Akt signaling pathway, Wnt-catenin formation, and Tyrosine metabolism. This founding indicated that most cancer-

related pathways were activated compared with normal tissue. KEGG analysis for all differentially expressed genes in KICH compared with normal tissue revealed TGF-beta signaling pathway, MAPK signaling pathway, cAMP signaling pathway, Chemical carcinogenesis, Cholesterol metabolism, Complement and coagulation cascades, and Cholesterol metabolism at the top cancer-related pathways, not disclosed in KIRC and KIRP(Supplemental Figure2E). Overall, these pathways and GO-terms results indicated that cell migration, cancer-related signal pathways play an important role in KICH.

3.2 CD8+ T cell infiltration in RCC is associated with the three subtypes

Based on the GO and KEGG analysis, the immune infiltration was found to be different in three subtypes. CD8+ cytolytic T cells (CTLs) recruitment also reflect immune cell infiltration by measuring CD8A expression. Immune cell cytolytic activity (CYT) by measuring the mRNA expression levels of granzyme A (GZMA) and perforin 1 (PRF1) are a prerequisite for effective antitumor killing. We obtained RNAseq from TCGA to explore if the CD8+ cytolytic T cell was associated with molecular subtypes. Interestingly, we found CD8A was highest in KIRC compared with the rest of two subtypes(Fig. 2B), meanwhile, the KIRP has a higher CD8+ cytolytic T cell infiltration relative to KICH, but CYT levels in KIRP was lower than KICH (Fig. 2B), so it's necessary to further explore. In addition, pathological type of RCC are found to have opposite trends in immune cell score and tumor purity based on ESTIMATE package of R(Fig. 2A), with tumor purity increasing from KIRC to KICH (KIRC<KIRP<KICH) and immune cell score decreasing from KIRC to KICH (KIRC> KIRP> KICH). In a short, these results may indicate that KIRC raised highest number of CD8+ T cell infiltration, while the KICH contained the lowest levels.

3.3 Distinct immune landscape associated with three subtypes in RCC

The different immune-related pathways and CD8+ T cell infiltration among the three subtypes of RCC make us to explore the immune landscape in three subtypes. The ssGSEA confirmed an expected main difference in expression of marker gene sets for immune landscape (Fig. 3A), including gradually increasing expression of marker gene sets for most of T cell subpopulations (CD4 and CD8 T cell, Natural killer T cell, Gamma delta T cell, Type 1 T helper cell, Regulatory T cell (treg), T follicular helper cell) from KICH to KIRC (KICH< KIRP< KIRC). Interestingly, Type 17 T helper cell was enriched highest level in KIRP, while this kind of subtype have lowest dense of Type 1 T helper cell relative to KIRC and KICH. In addition, some of innate immune cells including Macrophage, Mast cell, MDSC, Neutrophil, Activated and Immature dendritic cell were also gradually increasing from KICH to KIRC (KICH< KIRP< KIRC), exclusive of Eosinophil, Monocyte, CD56 natural killer cell, which suggest that the higher activation of effector and professional antigen-presenting immune process in KIRC. On the other hand, T cell priming and activity, including T cell co-stimulation, T cell co- inhibition and IFN expression also was explored based on ssGSEA (Fig. 3B). Besides, exhaustion T cell could indicate the immune process, especially immune evasion, we found KIRC has highest T cell exhaustion level according to gene sets (CTLA4, PD1, TIM3, LAG3, PDL1, and FASLG). Importantly, we found enrichment of T cell inflamed gene expression profiles

(Parainflammation and Inflammation), which could be used as a predictive of response to immunotherapy in tumor(Fig. 3C).

3.4 Differences in APC related to molecular subtypes

Dendritic cell (DC), as the most important antigen presenting cells (APC), play a critical role in innate immunity and adaptive new immunity, and as the only member of activating naïve T cell, DC has been paid more and more attention. We thus explored the process associated with DC maturation and T cell activation. From our above analysis, we found gradually increasing of immune signaling pathways and DC activation from KICH to KIRC. In addition, APC function could be reflected by the expression of gene sets including MHC Class I, HLA family, APC Co-inhibition, APC Co-stimulation and we observed the KIRC present highest levels compared with others(Fig. 4A). In addition, Pre-CDC differentiated into IRF4-dependent DC (IRF4-DC) and BATF3-dependent DC (BATF3-DC). Tissue DCS migrate to draining lymph nodes, where they show a mature phenotype, while the DCS stay in lymphoid organs always showed immature phenotype. The BARF3-DC development depends on the transcription factors IRF8 and BATF3, while the expression level RELB and IRF4 were critical to IRF4-DC mature (Fig. 4B). Our results reflected that the expression of BATF3-DC, LC, IRF4-DC signature were increasing from KICH to KIRC (KICH< KIRP< KIRC). Together, these results indicated KIRC was more closely associated with innate immune pathways and APC process which was critical to T cell activation.

3.5 The chemokine signatures difference among the three subtypes

Chemokines are increasingly recognized for their chemotactic effects, driving primed effector T cell recruitment into tumor, and the diversity of chemokine expression can mask the contribution of individual chemokine, then the 40 known human chemokines were explored in three subtypes respectively. We explored the relationship of all chemokines with cytolytic T cells in three subtypes(Fig. 5A), although active chemokines are similarity between KIRC and KIRP, we still found some chemokines were different, such as CXCL13 and CXCL16 which were more activity in immune response in KIRC than KIRP, while CCL25 and CXCL14 had the opposite trend. Previous report indicated that CXCL13/CXCR5 signaling modulates cancer cell ability to grow, proliferate, invade, and metastasize[22]. There are specific examples of chemokines important in lymphoid development, of which the CCL25-CCR9 axis plays a critical role in T cell development in thymus[23]. Our founding suggested that the different active chemokines between KIRC and KIRP may be critical biomarkers of the difference in immune mechanisms between them. The results also show that the active chemokines in KICH have huge variations compared with KIRC and KIRP, which indicated the immune response was different among them. When hematopoietic precursors from bone marrow colonize the thymus, the development of T cells in the thymus begins. Some chemokines participate in the seeding of the thymus rudiment by hematopoietic bone marrow precursors. Previous study found the CCR7 and CCR9, the ligands receptor of CCL19/CCL21 and CCL25, participate in this seeding process[24]. Interestingly, we found KIRC has higher the three chemokines infiltration compared with KIRP, while the KICH has the highest infiltration of CCL21 and

CCL25, thought above analysis found the CCL25 has lower correlation to cytolytic T cells, which mean that the KICH pay a more activity in this process [Fig. 5B].

More and more studies reported that multiple oncogenic mutations can affect the chemokine axes, which correlated with immune escape and tumor progress. The EGFR/Ras mutation in tumor cells induces a distinct chemokine repertoire, and tumors facilitate progression by the EGFR/Ras-induced production of CCL20[25]. From Supplemental Figure2, we found the Ras signal was more active in KICH, which may could explain the reason why the CCL20 was highest active in KICH than the two subtypes. In the other hand, the presence of T cells correlated with the expression of CCL2, CCL3, CCL4, CCL5, CXCL9, and CXCL10[26] and the cognate receptors of these chemokines were found to be upregulated on CD8+ effector T cells, then we explored these chemokines in three subtypes. The results indicated CCL2, CCL3, CCL4, and CCL5 were gradually increasing from KICH to KIRC, but CXCL9, CXCL10 and CXCL11 were significantly higher in KICH compared with KIRP (Fig. 5C). From figure 7D, the top 30 mutation genes were found based on the data from TCGA, and we found TP53, MUC4, PTEN, ZAN, TTN were the highest mutation frequency in KICH, while TTN, MUC16, MET, KMT2C, SETD2 in KIRP, and VHL, PBRM1, TTN, SETD2, BAP1 in KIRC. Previous study confirmed that PTEN loss in triple-negative breast cancer increased downstream production of IRF3 targets including CXCL10 expression level[27], which was consistent with our founding. CCR5, receptor of CCL5, CCL3 and CCL4, were elevated in BAP1-mutant clear cell renal cell carcinoma[28], which also explain why KIRC has a higher immune response. In conclusion, we found that oncogenic mutations can affect the chemokine activation in three subtypes, which could change the immune response.

3.6 The immune difference in molecular subtypes was replicated in independent studies

Based on expression levels of above gene sets used in TCGA, the three subtypes (KIRC, KIRP, KICH) present the immune infiltration landscape in public gene sets. The similar results were found in our validation datasets (GSE15641 and GSE19949/GSE12090), the two datasets all showed that KIRC has a higher immune score, while KICH has the lowest immune score (Fig. 6B). The heatmap of GSE15641 show significant different immune landscape of the three subtypes (Fig. 6A). In conclusion, the immune landscape was distinct in the subtypes, and the immune cell infiltration were increasing from KICH to KIRC (KICH< KIRP< KIRC).

3.7 Comparison to normal tissues suggested Cytotoxic lymphocytes activation in KIRC tumors only

In our data, compared with their paired normal tissue, we found B lineage and CD3+ T cells showed either no change or lower population of immune cell in three subtypes relative to their normal tissues (Supplemental Figure3). Interestingly, we found the CD8 T cell and Cytotoxic lymphocytes were significantly higher activation in KIRC while KIRP and KICH didn't show obvious activity relative to normal tissue. On the other hand, Monocytic lineage and Myeloid dendritic cells were more activity in KIRC and KIRP, though the latter is relatively lower, while the two kinds of immune cells have lower population of

immune cell in KICH. As for NK cells, though our above analysis confirmed that KICH has a lower infiltration relative to KIRP, NK cells was found to be more activity in KICH relative to their normal tissue.

Discussion

RCC subtypes patients with different cell types originating, as well as their histological, genetic and clinical diversity, may have different immue response. Therefore, accurate classification of RCC is crucial for targeted therapy selection. In order to find the unique genes signature in each subtype of RCC, we did RNA-seq analysis between KIRC, KIRP and KICH samples from TCGA. We identified 5699, 4896 and 5759 differentially expressed genes in KIRC, KIRP and KICH, respectively(Fig 1). The top upregulated genes including PAEP, HHATL and CRP in both subtypes of KIRC and KIRP play a major part in cancer progression. TERT, LHX9 and NKX6.1 were upregulated genes in KICH. Moreover, it was also noticed that UGT2A3, UGT3A1 and UGT1A9 from UGT family members were also significantly downregulation than normal tissues in KICH. UGT family could contribute to cancer risk by modulating the kidney exposure to mutagenic stimuli[29]. Expression changes of UGT family genes can affect the development and progression of various types of cancer including the cancer of the kidney cancer[30-33]. Moreover, it was also noticed that Cell migration and immune response process were enriched in KIRC and KIRP by GO and KEGG analysis(Supplemental Figure1,2). Furthermore, Compared to KICH, Th1 and Th2 cell differentiation, Chemokine signaling pathway, JAK-STAT signaling pathway and PI3K-Akt signaling pathway were more in KIRC, and p53 signaling pathway, cGMP-PKG signaling pathway, PI3K-Akt signaling pathway and Wnt-catenin formation in KIRP. But more synaptic plasticity and kidney morphogenesis were involved in KICH, and MAPK signaling pathway, cGMP-PKG signaling pathway in KICH. Our analyses clearly confirmed that KICH was a distinct disease that shared little genomic characteristics with KIRC and KIRP(Figure 1E,supplemental 4,5,6). Our study supported notion that Cells of origin were looked as one major determinant in the classification which reflecting molecular profiling differences of three subtypes. KIRC was thought to arise from cells in the proximal convoluted tubule, while KICH was thought to arise from intercalated cells in the distal convoluted tubule of the nephron, and KIRP was in general most similar to the proximal nephron. Our results suggested that KICH needed specific therapies, rather than simply adopting therapeutic strategies used for KIRC or KIRP.

Next, our results showed that three subtypes of RCC be different in the immune infiltration(Fig 2). CD8+ cytolytic T cells (CTLs) recruitment also reflect immune cell infiltration by measuring CD8A expression. We found that KIRC subtype was enriched not only in the highest number of immune cells(higher expression levels HLA genes and active CD4 T cell, active CD8 T cell and active B cell) (Fig 2,3,4), but also in many cancer-associated pathways including NF-kappa B signaling pathway, JAK-STAT signaling pathway and Cell cycle signaling pathway. Interestingly, we also fund PD-L1 and PD1 expression signaling showed significantly higher expression levels in KIRC (Fig 2, Supplemental Figure1). The Immunity High KIRP subtype contained in not only immune signatures, but also PI3K-Akt signaling pathway, Rap1 signaling pathway, Ras signaling pathway, MAPK signaling pathway, FoxO signaling pathway, JAK-STAT signaling pathway, HIF-1 signaling pathway, NF-kappa B signaling pathway and PD-L1 expression signaling. It were reported Resected RCC tumours were often extensively infiltrated by

CD8+ T cells, suggesting immune recognition of the tumour but poor tumour cell killing[34,35]. It may partially explain why an increased level of infiltrating CD8+ T cells was associated with worse outcome resulting from PD-L1 increased in tumor cell of KIRC and KIRP. Our studies suggested PD-L1 treatment would be most likely to have a good response in KIRC and KIRP patients. The KICH subtype was also enriched in TGF-beta signaling pathway, p53 signaling pathway, Hedgehog signaling pathway, EGFR tyrosine kinase inhibitor resistance, Notch signaling pathway, Hippo signaling pathway, Wnt signaling pathway, GnRH signaling pathway, VEGF signaling pathway, AMPK signaling pathway, cGMP-PKG signaling pathway and mTOR signaling pathway. Interestingly, we found that the TGF signaling pathway had a significantly enrichment in KICH subtype, this observation was in agreement with findings from previous studies showing that the TGF signaling pathway plays a key role in preventing PD-L1 treatment[36]. Although PD-L1 inhibitor showed its efficacy in KIRC and KIRP patients treated with pembrolizumab, the efficacy of immune checkpoint inhibitors in metastatic KICH is low, as no responses were observed[37-39]. Sanjeev reported TGF-β signaling resulted in exclusion of T cells by the stromal barrier limits, and TGF-β inhibition potentiated the ability of anti–PD-L1 to enhance anti-tumour immunity resulting in optimal T cell positioning[39]. Our studies suggested co-inhibition of TGF-β and PD-L1 may be good applicable to KICH. Moreover, we firstly found the higher infiltration of CCL21 and CCL25 in the KICH compared to KIRC and KIRP(Fig 5), CCL21 and CCL25 signaling was proved not only promoting proliferation, invasion, migration and drug-resistance in several types of tumors, but also inducing immune evasion[40-42]. Our data hinted CCL21 and CCL25 might be a potential target for KICH therapy. Besides, KICH exhibited more active stem cell-associated biological processes(Notch, Hippo and Wnt signaling pathway) than KIRC and KIRP subtypes. However, its mechanism in KICH needs to be further studied.

Previous reports have indicated that the somatic genes mutation regulation that disrupts the function of tumor suppressor genes or oncogenes and was shown to promote carcinogenesis with the alteration of immune signature genes that can significantly effect on immunotherapy [43-47]. Thus, We next sought to identify mutation that were specifically associated with immune in KICH, KIRC, and KIRP. In our studies, the mutation genes were completely different in the top 30 mutated genes in three subtypes of RCC. Firstly, we found the VHL and PBRM1 were the most mutation frequency genes in KIRC. It was known that VHL somatic mutation or deletion was characteristic of most KIRC[48]. Loss of VHL usually induce cellular proliferation and promote angiogenesis by actived HIF and STAT3 signal, and STAT3 increased PD-L1 expression in transcriptional level[49,50]. Furthermore, We noticed SWI/SNF complex genes including PBRM1, ARID1A and SMARCA4 were high mutation frequency in KIRC and KIRP. Loss ARID1A or PBRM1-deficient elevated PD-L1 expression in tumor cell [51-52]. MET, SRRM2 and WDFY3 was higher mutation frequency in KIRP. Loss SRRM2 and WDFY3 reduced immue cell differentiation[53,54]. Another interesting founding was that TTN, MUC16, MET, KMT2C were the most mutation frequency genes. In KICH, the vast majority of patients harboured mutations in TP53 and PTEN, which was previously reported as the most frequency mutated gene. MUC4, AGAP4, ZAN, TTN, FAT3, FLT4, and SETD1B mutation was found in KICH, most of which have been reported to be associated with cancer process.

These results suggested that the mutation can be used to distinguish patients with different sensitivities to immunotherapy, making individualized treatment strategies a possibility.

Conclusions

In summary, Understanding the genetic features and immune signature-based classification of RCC subtypes will provide effective stratification of therapy for patients responsive to immunotherapy. Our studies had yielded several important conclusions: KICH was a distinct disease that shared little genomic characteristics with KIRC and KIRP. It is imaginable that patients with KIRC and KIRP would be more likely to respond to anti-PD-1/ PD-L1 therapy than patients with KICH subtype. It was better choose with TGF inhibitor adding PD-L1 inhibitor therapy in KICH. It was unexpected discovery that CCL21 and CCL25 might be a potential target for KICH therapy. Additionally, our study can stratify patients with different mutation and help to predict the sensitivity of patients to immunotherapy.

Abbreviations

RCC: Renal cell carcinomas; KIRC: clear cell RCC; KIRP: papillary RCC; KICH: chromophobe RCC; TCGA: The Cancer Genome Atlas; MAPKs: Mitogen-activated protein kinases; ICIs: immune checkpoint inhibitors; PD-L1: programmed death ligand 1; TMB:tumor mutation burden; GO: Gene ontology; WGCNA: weighted gene co-expression network analysis;

Declarations

Acknowledgements

We would like to thank other members in the lab for discussion and suggestions.

Authors' contributions

Ning Jiang and Xin Lou conceived of the study and carried out its design. Ning Jiang, Jianing Guo, Xi Yu, Xiaofei Lv, Bin He, Pu Wang and Shenglai Liu collected TCGA data. Jianing Guo analyzed the data, Jianing Guo and Jiang Ning wrote the paper. All authors read and approved the final manuscript.

Funding: This work was supported by grants from the National Natural Science Foundation (81872079, 81572538), and the Science Foundation of Tianjin (No.:11JCZDJC19700,16JCZDJC34400,14JCYBJC26300), 20140117,16KG118.

Availability of data and materials

All data generated or analyzed during this study are included in this article.

Consent for publication

All subjects have written informed consent

Conflict of Interest

None of the authors have any relevant conflicts of interest pertaining to the studies and data in this manuscript.

Ethics approval and consent to participate

Not applicable

References

1. Siegel RL, Miller KD, Fuchs HE et al (2021) Cancer Statistics, 2021. CA Cancer J Clin 71:7–33
2. Rossi SH, Klatte T, Usher-Smith J et al (2018) Epidemiology and screening for renal cancer. World J Urol 36:1341–1353
3. Linehan WM, Ricketts CJ (2019) The Cancer Genome Atlas of renal cell carcinoma: findings and clinical implications. Nat Rev Uro 16:539–552
4. Graham J, Dudani S, Heng DYC (2018) Prognostication in Kidney Cancer: Recent Advances and Future Directions. J Clin Oncol 29:JCO2018790147
5. Hsieh JJ, Purdue MP, Signoretti S et al (2017) Renal cell carcinoma. Nat Rev Dis Primers 3:17009
6. Chen Y, Liu Q, Chen Z et al (2019) PD-L1 expression and tumor mutational burden status for prediction of response to chemotherapy and targeted therapy in non-small cell lung cancer. J Exp Clin Cancer Res 38:193
7. Brian I, Rini T, Powles MB, Atkins et al (2019) Atezolizumab plus bevacizumab versus sunitinib in patients with previously untreated metastatic renal cell carcinoma (IMmotion151): a multicentre, open-label, phase 3, randomised controlled trial. Lancet 393:2404–2415
8. Robert J, Motzer K, Penkov J, Haanen et al (2019) Avelumab plus Axitinib versus Sunitinib for Advanced Renal-Cell Carcinoma. N Engl J Med 380:1103–1115
9. David F, McDermott, Mahrukh A, Huseni MB, Atkins et al (2018) Clinical activity and molecular correlates of response to atezolizumab alone or in combination with bevacizumab versus sunitinib in renal cell carcinoma. Nat Med 24:749–757
10. Toni K, Choueiri J, Larkin M, Oya et al (2018) Preliminary results for avelumab plus axitinib as first-line therapy in patients with advanced clear-cell renal-cell carcinoma (JAVELIN Renal 100): an open-label, dose-finding and dose-expansion, phase 1b trial. Lancet Oncol 19:451–460
11. Sharma P, Retz M, Siefker-Radtke A et al (2017) Nivolumab in metastatic urothelial carcinoma after platinum therapy (CheckMate 275): a multicentre, single-arm, phase 2 trial. Lancet Oncol 18:312–322
12. Motzer RJ, Rini BI, McDermott DF et al (2019) Nivolumab plus ipilimumab versus sunitinib in first-line treatment for advanced renal cell carcinoma: extended follow-up of efficacy and safety results from

a randomised, controlled, phase 3 trial. Lancet Oncol 20:1370–1385
13. Motzer RJ, Tannir NM, McDermott DF et al (2018) Nivolumab plus Ipilimumab versus Sunitinib in Advanced Renal-Cell Carcinoma. N Engl J Med 378:1277–1290
14. Clark JI, Wong MKK, Kaufman HL et al (2017) Impact of Sequencing Targeted Therapies With High-dose Interleukin-2 Immunotherapy: An Analysis of Outcome and Survival of Patients With Metastatic Renal Cell Carcinoma From an On-going Observational IL-2 Clinical Trial: PROCLAIMSM. Clin Genitourin Cancer 15:31–41
15. Rizvi NA, Hellmann MD, Snyder A et al (2015) Cancer immunology. Mutational landscape determines sensitivity to PD-1 blockade in non-small cell lung cancer. Science 348:124–128
16. Hugo W, Zaretsky JM, Sun L et al (2016) Genomic and Transcriptomic Features of Response to Anti-PD-1 Therapy in Metastatic Melanoma. Cell 165:35–44
17. Van Allen EM, Miao D, Schilling B et al (2015) Genomic correlates of response to CTLA-4 blockade in metastatic melanoma. Science 350:207–211
18. Le DT, Uram JN, Wang H et al (2015) PD-1 Blockade in Tumors with Mismatch-Repair Deficiency. N Engl J Med 372:2509–2520
19. Guangchuang Yu L-G, Wang Y, Han et al (2012) clusterProfiler: an R package for comparing biological themes among gene clusters. OMICS 16:284–287
20. Qingzhu Jia W, Wu Y, Wang et al (2018) Local mutational diversity drives intratumoral immune heterogeneity in non-small cell lung cancer. Nat Commun 9:5361
21. Kosuke Yoshihara M, Shahmoradgoli E, Martínez et al (2013) Inferring tumour purity and stromal and immune cell admixture from expression data. Nat Commun 4:2612
22. Etienne Becht, Nicolas A, Giraldo L, Lacroix et al (2016) Estimating the population abundance of tissue-infiltrating immune and stromal cell populations using gene expression. Genome Biol 17:218
23. Vicari AP, Figueroa DJ, Hedrick JA et al (1997) TECK: a novel CC chemokine specifically expressed by thymic dendritic cells and potentially involved in T cell development. Immunity 7:291–301
24. Krueger A, Willenzon S, Lyszkiewicz M et al (2010) CC chemokine receptor 7 and 9 double-deficient hematopoietic progenitors are severely impaired in seeding the adult thymus. Blood 115:1906–1912
25. Hippe A, Braun SA et al (2020) EGFR/Ras-induced CCL20 production modulates the tumour microenvironment. Br J Cancer 30. doi: 10.1038/s41416-020-0943-2
26. Helena Harlin Y, Meng AC, Peterson et al (2009) Chemokine expression in melanoma metastases associated with CD8+ T-cell recruitment. Cancer Re 69:3077–3085
27. Jessica L, Ritter Z, Zhu, Tran C, Thai et al (2020) Phosphorylation of RAB7 by TBK1/IKKε Regulates Innate Immune Signaling in Triple-Negative Breast Cancer. Cancer Res 80:44–56
28. Quan Zhou Y, Qi Z, Wang et al (2020) CCR5 blockade inflames antitumor immunity in BAP1-mutant clear cell renal cell carcinoma. J Immunother Cancer 8:e000228
29. Margaillan G, Rouleau M, Fallon JK et al (2015) Quantitative profiling of human renal UDP-glucuronosyltransferases and glucuronidation activity: a comparison of normal and tumoral kidney

tissues. Drug Metab Dispos 43:611–619

30. Tang D, Zhao YC, Liu H et al (2020) Potentially functional genetic variants in PLIN2, SULT2A1 and UGT1A9 genes of the ketone pathway and survival of nonsmall cell lung cancer. Int J Cancer 18. doi: 10.1002/ijc.32932
31. Yang ZZ, Li L, Wang L et al (2017) The regioselective glucuronidation of morphine by dimerized human UGT2B7, 1A1, 1A9 and their allelic variants. Acta Pharmacol Sin 38:1184–1194
32. De Mattia E, Cecchin E, Polesel J et al (2017) UGT1A polymorphisms as genetic biomarkers for hepatocellular carcinoma risk in Caucasian population. Liver Int 37:1345–1353
33. Calvo N, Shabaka A, Rodriguez Cubillo B et al (2016) Presence of T-275A and C-2152T Polymorphisms of the Promoter Region of Uridine Diphosphate-Glucuronosyltransferase 1A9 Increases Mortality From Digestive Tumors: Results After 10 Years of Follow-up in a Renal Transplant Population. Transplant Proc 48:2947–2949
34. Siska PJ, Beckermann KE, Mason FM et al (2017) Mitochondrial dysregulation and glycolytic insufficiency functionally impair CD8 T cells infiltrating human renal cell carcinoma. *JCI Insight* 2:pii: 93411
35. Giraldo NA, Becht E, Pagès F et al (2015) Orchestration and Prognostic Significance of Immune Checkpoints in the Microenvironment of Primary and Metastatic Renal Cell Cancer. Clin Cancer Res 21:3031–3040
36. Sanjeev Mariathasan SJ, Turley D, Nickles et al (2018) TGFβ attenuates tumour response to PD-L1 blockade by contributing to exclusion of T cells. Nature 554:544–548
37. Rini BI, Plimack ER, Stus V et al (2019) Pembrolizumab plus Axitinib versus Sunitinib for Advanced Renal-Cell Carcinoma. N Engl J Med 380:1116–1127
38. Koshkin VS, Barata PC, Zhang T et al (2018) Clinical Activity of Nivolumab in Patients With Non-Clear Cell Renal Cell Carcinoma. J Immunother Cancer 6:9
39. Rana RMcKay, Bossé D, Xie W et al (2018) The Clinical Activity of PD-1/PD-L1 Inhibitors in Metastatic Non-Clear Cell Renal Cell Carcinoma. Cancer Immunol Res 6:758–765
40. Jacqueline D, Shields, Iraklis C, Kourtis, Alice A, Tomei et al (2010) Induction of lymphoidlike stroma and immune escape by tumors that express the chemokine CCL21. Science 328:749–752
41. Balsam, Rizeq, Mohammed Imad Malki (2020) The Role of CCL21/CCR7 Chemokine Axis in Breast Cancer Progression. Cancers (Basel) 12:1036
42. Yuxu Niu D, Tang L et al (2020) CCL25 promotes the migration and invasion of non-small cell lung cancer cells by regulating VEGF and MMPs in a CCR9-dependent manner. Exp Ther Med 19:3571–3580
43. Le DT, Uram JN, Wang H et al (2015) PD-1 Blockade in Tumors with Mismatch-Repair Deficiency. *N Engl J Med*. 2015;372,2509-20
44. Rizvi NA, Hellmann MD, Snyder A et al (2015) Cancer immunology. Mutational landscape determines sensitivity to PD-1 blockade in non-small cell lung cancer. Science 348:124–128

45. Huang AC, Postow MA, Orlowski RJ et al (2017) T-cell invigoration to tumour burden ratio associated with anti-PD-1 response. Nature 545:60–65
46. Samstein RM, Lee CH, Shoushtari AN et al (2019) Tumor mutational load predicts survival after immunotherapy across multiple cancer types. Nat Genet 51:202–206
47. Yarchoan M, Hopkins A, Jaffee EM (2017) Tumor Mutational Burden and Response Rate to PD-1 Inhibition. N Engl J Med 377:2500–2501
48. Wang L, Liang Y, Li P et al (2019) Oncogenic Activities Of UBE2S Mediated By VHL/HIF-1α/STAT3 Signal Via The Ubiquitin-Proteasome System In PDAC. Onco Targets Ther 12:9767–9781
49. Li P, Huang T, Zou Q et al (2019) FGFR2 Promotes Expression of PD-L1 in Colorectal Cancer via the JAK/STAT3 Signaling Pathway. J Immunol 202:3065–3075
50. Shen J, Ju Z, Zhao W et al (2018) ARID1A deficiency promotes mutability and potentiates therapeutic antitumor immunity unleashed by immune checkpoint blockade. Nat Med 24:556–562
51. Huang Y, Wang J, Jia P et al (2019) Clonal architectures predict clinical outcome in clear cell renal cell carcinoma. Nat Commun 10:1245
52. Miao D, Margolis CA, Gao W et al (2018) Genomic correlates of response to immune checkpoint therapies in clear cell renal cell carcinoma. Science 359:801–806
53. Naito T, Udagawa H, Umemura S et al (2019) Non-small cell lung cancer with loss of expression of the SWI/SNF complex is associated with aggressive clinicopathological features, PD-L1-positive status, and high tumor mutation burden. Lung Cancer 138:35–42
54. Youn HG, Matsumoto J, Tanaka Y et al (2003) SR-related protein TAXREB803/SRL300 is an important cellular factor for the transactivational function of human T-cell lymphotropic virus type 1 Tax. J Viro 77:10015–10027

Table

Table 1. Patient baseline characteristics

Characteristic	HCC patents (n=1012)
Age, year (mean±SD)	60.2±12.5
Male, n (%)	681(68.2%)
Race (White), n (%)	830(80.2%)
Smoking, PY (mean ± SD)	30.7±24.9
Laterality(left), n (%)	501 (49.5%)
Kidney Chromophobe (KICH), n (%)	85(8.4%)
Kidney Clear Cell Carcinoma (KIRC), n (%)	606(59.9%)
Kidney Papillary Cell Carcinoma (KIRP), n (%)	321(31.7%)
Positive Lymph node metastasis (LN+)	452 (44.6%)
Stage, n (%)	
I	513(50.2%)
II	123(12.0%)
III	215(21.2%)
IV	129(12.7%)
Deaths (%)	263(30.1%)

Supplemental Figures

Supplemental Figures S1-S3 are not available with this version

Figures

Figure1

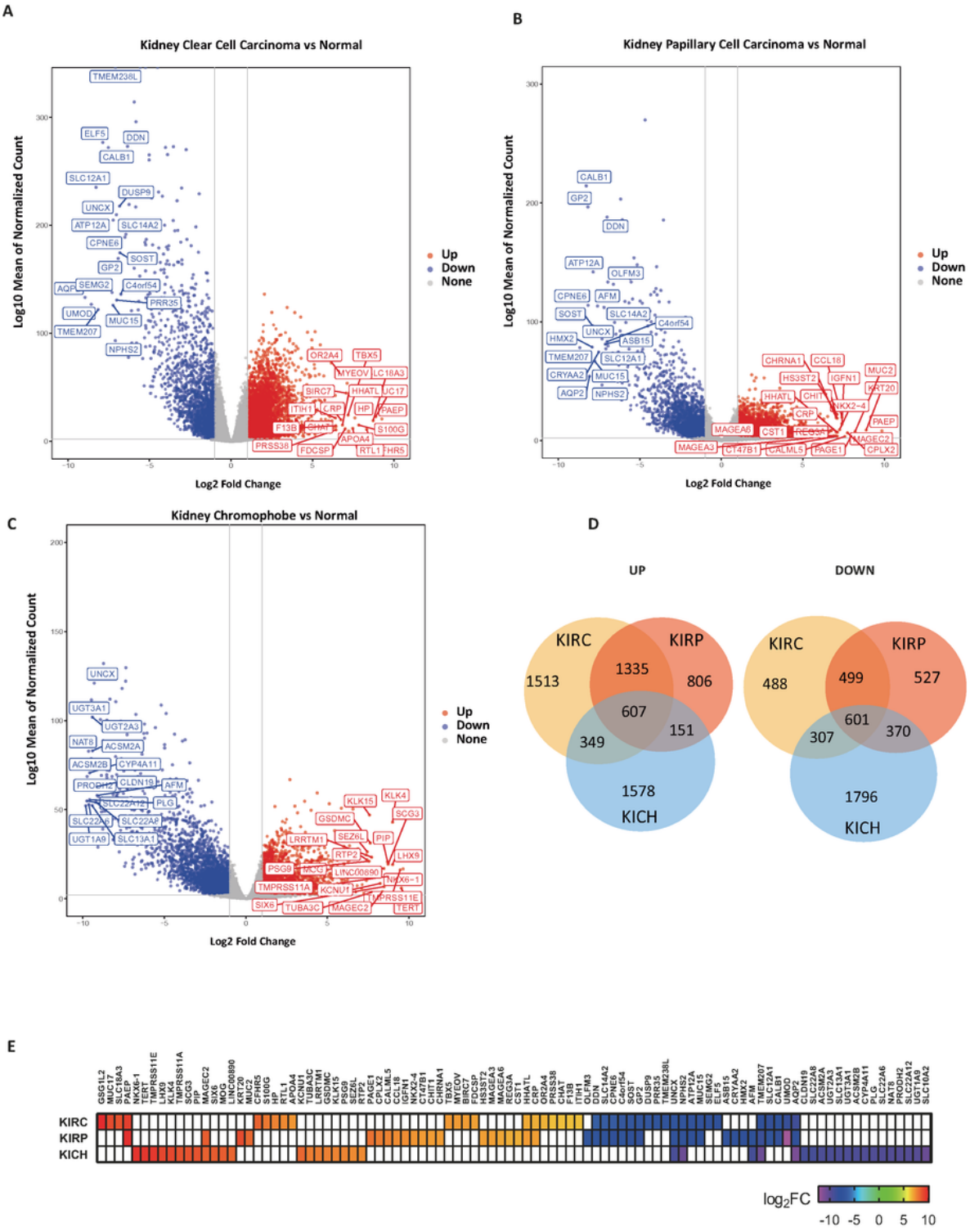

Figure 1

Differential gene expression in Kidney Chromophobe (KICH), Kidney Clear Cell Carcinoma (KIRC), Kidney Papillary Cell Carcinoma (KIRP).

(A). Volcano plot of differentially expressed genes (DEGs) in KIRC subtype of Renal cell carcinomas (RCC). The horizontal line at false discovery rate (FDR) = 0.01; vertical line at |log2FC|=1; (B) Volcano plot

of differentially expressed genes (DEGs) in KIRP subtype of RCC. (C) Volcano plot of differentially expressed genes (DEGs) in KICH subtype of RCC. (D) Venn diagram shows overlap among differentially expressed genes in KICH, KIRC, and KIRP. Up-regulated and down-regulated genes between tumor and normal tissue were shown respectively. (E) top 20 genes up- and down-regulation in KIRC, KRP and KICH tissue compared with normal tissue. In the heatmap indicate log fold change (FC), the color white represent missing value.

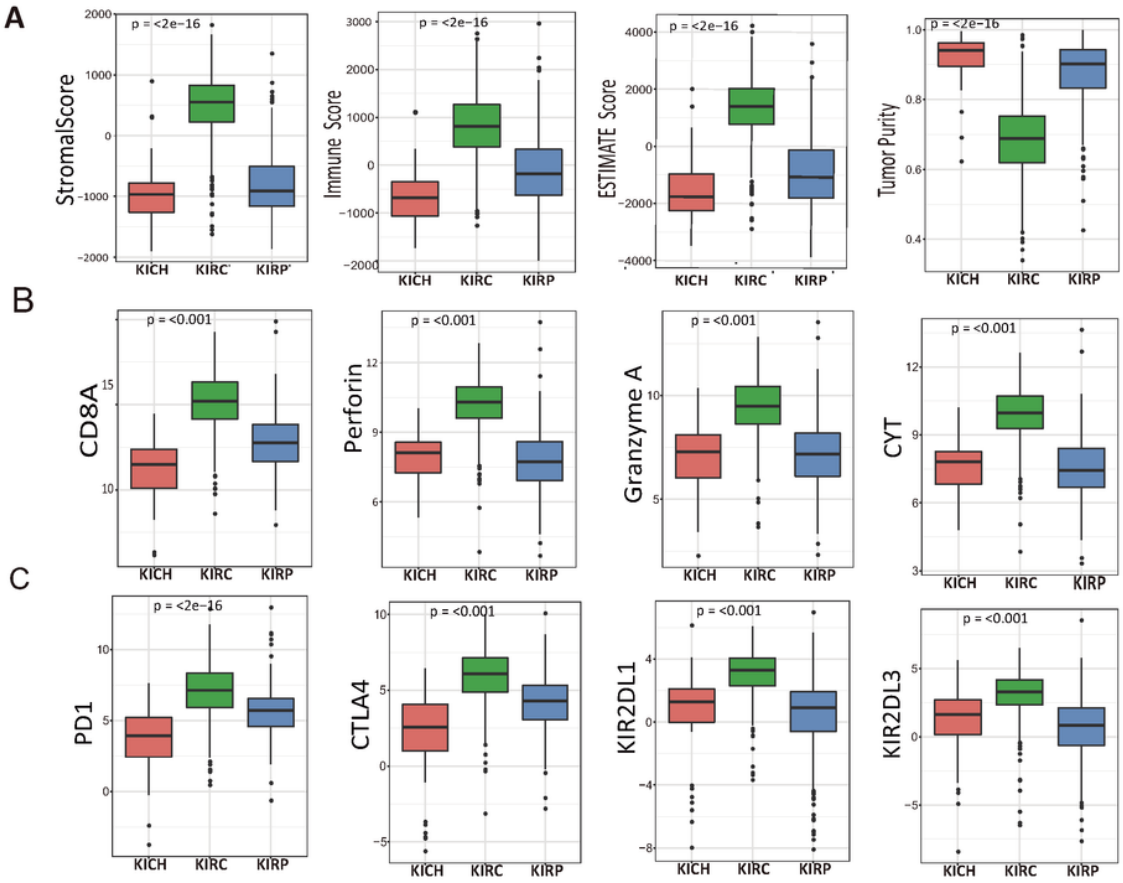

Figure 2

CD8+ T cell infiltration levels exploration in the three subtypes.

(A) the immune cell infiltration level (immune score), tumor purity, and stromal score among KICH, KIRC and KIRP. (B) CD8+ cytolytic T cells, Granzyme B, Perforin, and immune cell cytolytic activity (CYT) among KICH, KIRC, and KIRP. (C) The immune checkpoint expression of PD1, CTLA-4 and the expression of killer cell immunoglobulin-like receptor inhibitory genes among KICH, KIRC, and KIRP.

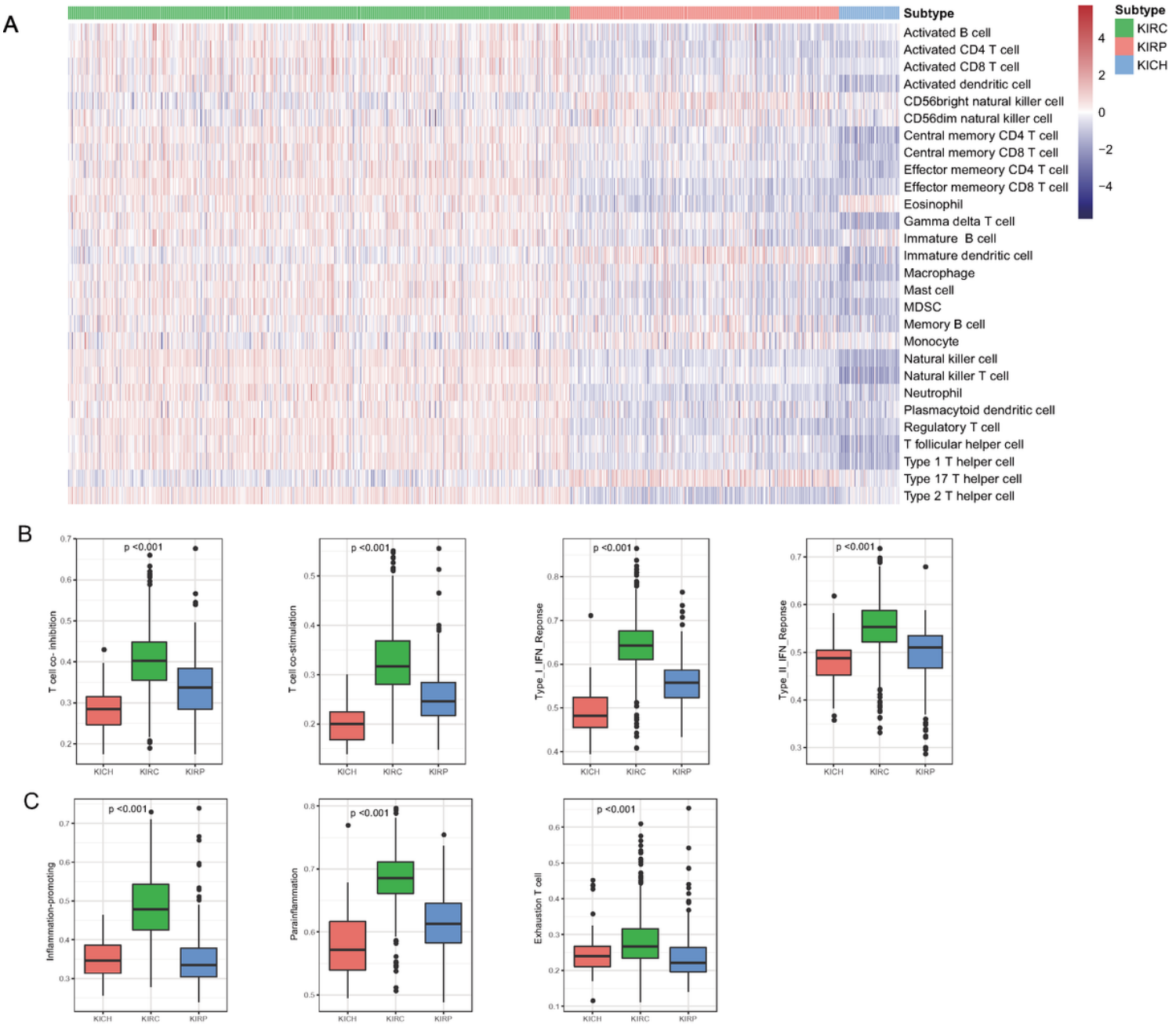

Figure 3

Immune landscape associated with three subtypes in RCC

(A)Heatmap of ssGSEA scores of 28 gene sets indicative of immune cell populations in the three subtypes (KIRC, KIRP, KICH). (B) Boxplot of ssGSEA scores of gene sets characteristic of immune responses related to T cell activation among three subtypes. (C) Boxplot of ssGSEA scores of T cell inflammation signatures (Parainflammation and Inflammation-promoting) among three subtypes; Boxplot of ssGSEA scores differences of T cell exhaustion genes among three subtypes.

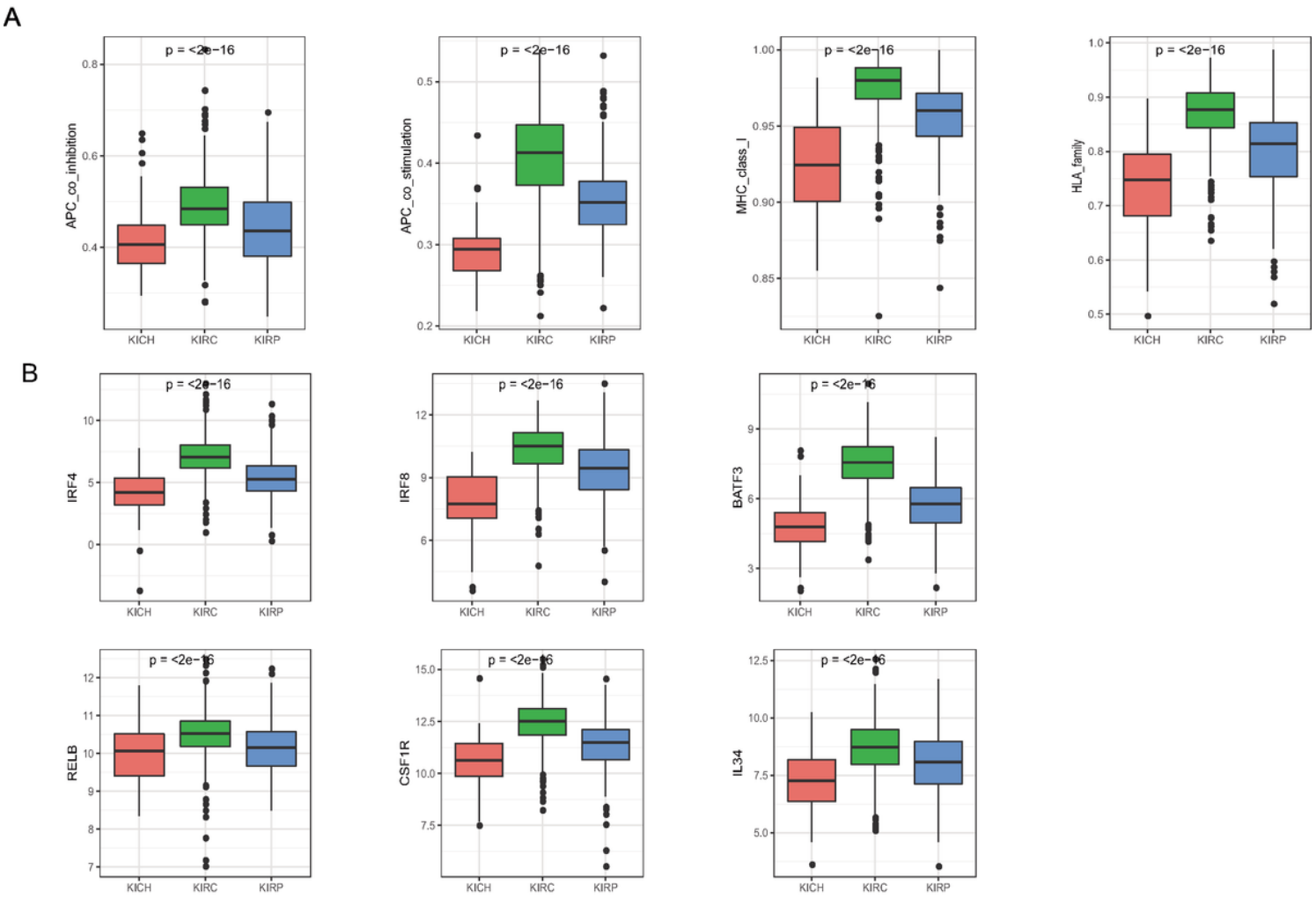

Figure 4

Hallmarks of professional APC activation related to the three subtypes

(A)Boxplot of ssGSEA scores of gene sets in immune responses involved with APC activation (co_inhibition APC, co_stimulation APC, MHC class_I, HLA family) among three subtypes. (B) Differences in biomarker expression of the BATF3-DC and IRF4-DC.

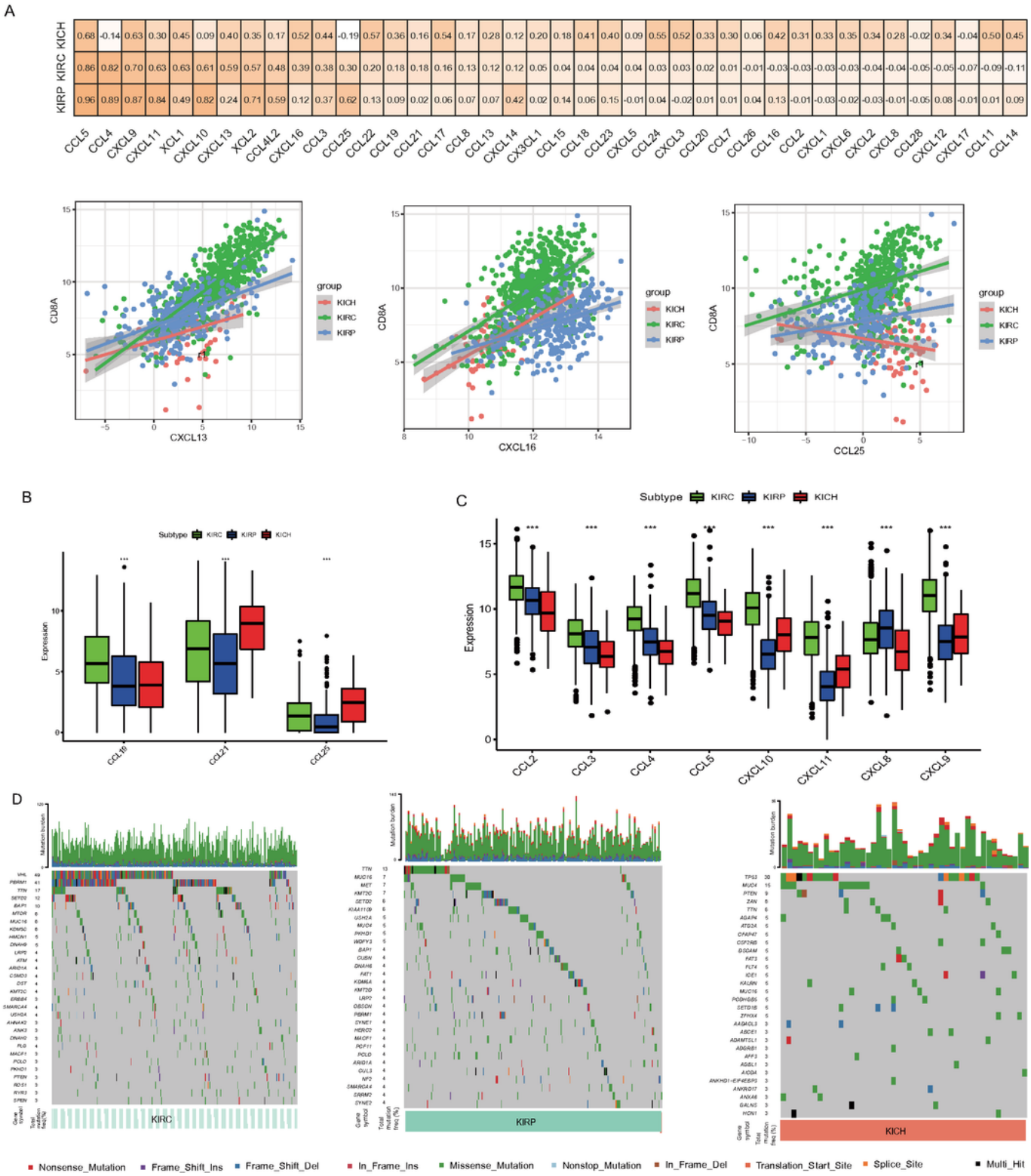

Figure 5

The chemokine signatures difference among the three subtypes

(A)Correlation between chemokine expression with CD8A levels among three subtypes, and the correlation coefficients (R2) were shown in each small cells; The Scatter plots shown that special expression of CXCL13, CXCL16, CCL25 were associated with CD8A. (B) Boxplot of expression of CCL19,

CCL21, CCL25 among three subtypes. (C) Boxplot of expression of CCL2, CCL3, CCL4, CCL5, CXCL9, and CXCL10 among three subtypes. (D) Mutational landscape among three subtypes; Genes with top 30 mutation frequency in each subtype is presented on the right. The mutation load for each sample is presented above the mutation plot

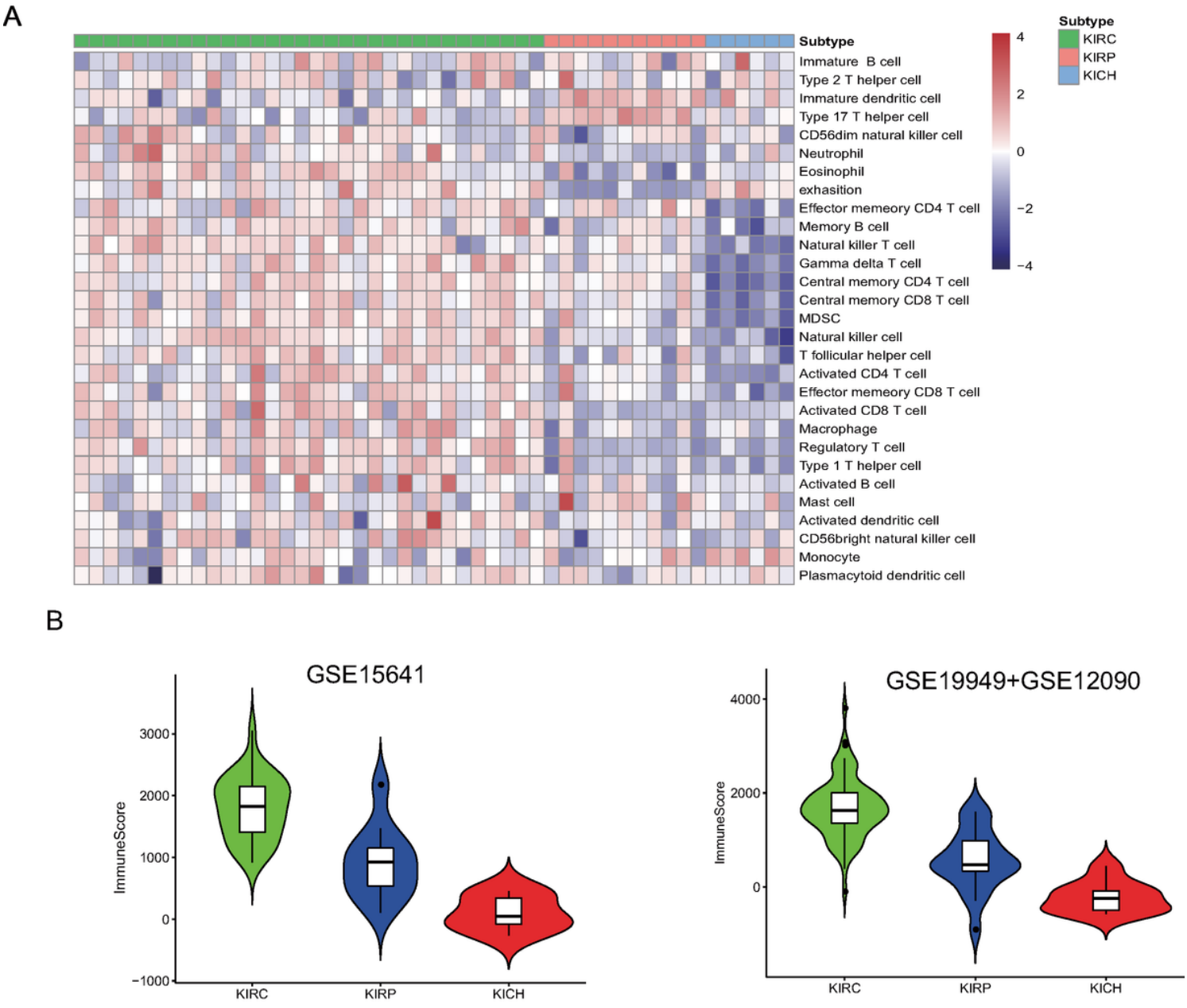

Figure 6

immune landscape in three subtypes was validated in independent datasets

(A) Heatmap of ssGSEA scores of 28 gene sets indicative of immune cell populations in the three subtypes based on dataset (GSE15641). (B) Comparison of the immune cell infiltration levels among three subtypes based on two datasets.